British Journal of Pharmacology

DOI:10.1111/j.1476-5381.2011.01624.x
www.brjpharmacol.org

RESEARCH PAPER

Expression, assembly and function of novel C-terminal truncated variants of the mouse P2X7 receptor: re-evaluation of P2X7 knockouts

Correspondence
Ruth Murrell-Lagnado, Department of Pharmacology, University of Cambridge, Tennis Court Road, Cambridge CB2 1PD, UK. E-mail: rdm1003@cam.ac.uk

*Joint senior authors.

Keywords
mouse P2X7 receptors; splice variants; P2X7$^{-/-}$ mice

Received
17 March 2011
Revised
5 July 2011
Accepted
18 July 2011

Marianela Masin[1], Christopher Young[2], KoiNi Lim[2], Sara J Barnes[1], Xing Jian Xu[1], Viola Marschall[1], Wojciech Brutkowski[2], Elizabeth R Mooney[1], Dariusz C Gorecki[2]* and Ruth Murrell-Lagnado[1]*

[1]*Department of Pharmacology, University of Cambridge, Cambridge, UK, and* [2]*School of Pharmacy and Biomedical Sciences, University of Portsmouth, Portsmouth, UK*

BACKGROUND AND PURPOSE

Splice variants of P2X7 receptor transcripts contribute to the diversity of receptor-mediated responses. Here, we investigated expression and function of C-terminal truncated (ΔC) variants of the mP2X7 receptor, which are predicted to escape inactivation in one strain of P2X7$^{-/-}$ mice (Pfizer KO).

EXPERIMENTAL APPROACH

Expression in wild-type (WT) and Pfizer KO tissue was investigated by reverse transcription (RT)-PCR and Western blot analysis. ΔC variants were also cloned and expressed in HEK293 cells to investigate their assembly, trafficking and function.

KEY RESULTS

RT-PCR indicates expression of a ΔC splice variant in brain, salivary gland (SG) and spleen from WT and Pfizer KO mice. An additional ΔC hybrid transcript, containing sequences of P2X7 upstream of exon 12, part of exon 13 followed in-frame by the sequence of the vector used to disrupt the P2X7 gene, was also identified in the KO mice. By blue native (BN) PAGE analysis and the use of cross linking reagents followed by SDS-PAGE, P2X7 trimers, dimers and monomers were detected in the spleen and SG of Pfizer KO mice. The molecular mass was reduced compared with P2X7 in WT mice tissue, consistent with a ΔC variant. When expressed in HEK293 cells the ΔC variants were inefficiently trafficked to the cell surface and agonist-evoked whole cell currents were small. Co-expressed with P2X7A, the ΔC splice variant acted in a dominant negative fashion to inhibit function.

CONCLUSIONS AND IMPLICATIONS

Pfizer KO mice are not null for P2X7 receptor expression but express ΔC variants with reduced function.

Abbreviations

Ab, antibody; BzATP (2′(3′)-*O*-(4-benzoylbenzoyl)adenosine-5′-triphosphate); KO, knockouts; SG, salivary gland

Introduction

ATP is an important extracellular signalling molecule, which acts upon two distinct classes of receptors that differ in their mode of action: P2X, being ionotropic, and P2Y, being metabotropic receptors (receptor nomenclature follows Alexander *et al.*, 2011). The P2X receptors function as homo- and heterotrimers of subunits, both their N- and C-termini being intracellular with the two transmembrane domains connected by a large extracellular loop (Murrell-Lagnado and Qureshi, 2008). The seven members (P2X1–7) of this family, in response to binding ATP, all open a non-selective cation

channel highly permeable to calcium, but they differ in their tissue distribution, pharmacology and biophysical properties (North, 2002). The P2X7 receptor is structurally and functionally distinct from the other members of this family in that it has an extended carboxy-terminal domain, ~240 amino acids in length, which is involved in interactions with other proteins and lipids (Roberts *et al.*, 2006). It has relatively low affinity for ATP compared with the other members of this family, and upon sustained activation, it triggers membrane permeabilization to large molecules up to 900 Da (Di Virgilio, 1995). In addition it activates a diverse range of cellular responses, including activation of phospholipase A2, phospholipase D, mitogen-activated protein kinase and NF-κB (Humphreys and Dubyak, 1996; Ferrari *et al.*, 1997b; Armstrong *et al.*, 2002). The C-terminal domain of the receptor is crucial for membrane permeabilization, transduction and signalling (Gu *et al.*, 2001; Adriouch *et al.*, 2002; Armstrong *et al.*, 2002; Smart *et al.*, 2003; Wiley *et al.*, 2003).

P2X7 is expressed predominantly in cells of hematopoietic lineage (Surprenant *et al.*, 1996), including macrophages, microglia and lymphocytes. Here, it triggers the processing and release of proinflammatory cytokines and promotes phagocytosis, the killing of mycobacteria and apoptosis (Ferrari *et al.*, 1997a; MacKenzie *et al.*, 2001; Sanz and Di Virgilio, 2000; Gu *et al.* 2010). It is also expressed in other cell types including epithelia, endothelia and neurons in the CNS (Surprenant and North, 2009) and its properties differ in a cell type-dependent manner; for example, P2X7-triggered membrane permeabilization to large molecules such as fluorescent dyes does not occur in all cells expressing this receptor. Also, in some instances, the activation of P2X7 promotes cell survival and proliferation, rather than cell death (Adinolfi *et al.*, 2005). Although the nature of the response is partly dependent upon the agonist concentrations used, there might also be cell type-dependent differences in the molecular composition of the P2X7 receptor complex. Several other proteins have been identified that interact with the P2X7 receptor, including the P2X4 receptor (Guo *et al.*, 2007; Boumechache *et al.*, 2009; Antonio *et al.*, 2011) and the pannexin-1 hemichannel (Pelegrin and Surprenant, 2006). Also splice variants have been identified for both the human and mouse isoforms of P2X7, which differ in their functional properties from the full-length P2X7A receptor (Cheewatrakoolpong *et al.*, 2005). For human P2X7 receptors, one of the splice variants contains a large C-terminal deletion (ΔC), and is prevalent and functional. A recent study showed that this variant is able to mediate calcium influx and membrane depolarization but can no longer trigger membrane permeabilization to larger molecules (Adinolfi *et al.*, 2010). Importantly it can still activate NF-κB and promote cell survival and proliferation. Another splice variant, containing a larger deletion at the C-terminus and lacking TM2, was expressed in cervical cancer cells, was non-functional and acted in a dominant negative fashion to disrupt the normal paracrine/autocrine ATP signalling, thereby contributing to dysregulated cell proliferation (Feng *et al.*, 2006).

For the mouse P2X7 receptor, a novel splice variant utilizing an alternative exon 1, encoding the N-terminus and part of TM1, was recently identified (P2X7K) (Nicke *et al.*, 2009). This is of interest for several reasons: it has higher sensitivity to agonist than the original P2X7A receptor; it rapidly triggers membrane permeabilization as measured by ethidium uptake; it is expressed more selectively, particularly in spleen lymphocytes; and it escapes inactivation in one of the commonly used strain of $P2X7^{-/-}$ mice (Glaxo). There are two strains of mice in which the P2X7 gene has been disrupted: one is from Glaxo, which has a LacZ gene and neomycin cassette (Neo) inserted into exon 1 and the other from Pfizer which has a Neo insertion in exon 13 (Solle *et al.*, 2001; Sim *et al.*, 2004). While experiments with these mice have identified several important roles for P2X7 both in physiological and pathological states, including neurodegeneration, inflammation and neuropathic pain (Labasi *et al.*, 2002; Ke *et al.*, 2003; Chessell *et al.*, 2005; Khakh and North, 2006; Hughes *et al.*, 2007), there are some key differences reported for the two knockout (KO) strains, which were initially unexplained. For example, macrophages from the Pfizer KO mice show a large reduction in ATP-stimulated IL-6 production, whereas the macrophages from Glaxo KO mice showed a very large enhancement in IL-6 production (Chessell *et al.*, 2005). In a mouse model of multiple sclerosis, the Pfizer KO mice showed exacerbation of disease. In contrast, the Glaxo mice showed a reduction in the incidence of disease (Sharp *et al.*, 2008). The splenic T cells from the Glaxo mice surprisingly produced greater IFN-γ and IL-17 release than the WT cells, and enhanced P2X7 receptor-mediated responses were found in T lymphocytes from the Glaxo KO mice compared with WT cells (Taylor *et al.*, 2009). Moreover, controversies surrounding P2X7 receptor extend to its expression and function in the CNS neurons. There are reports that show P2X7 receptors in presynaptic terminals and their involvement in modulating excitatory synaptic transmission. However, neuronal P2X7 immunoreactivity is also present in the KO mice and P2X7-like calcium responses were recorded from cultured cerebellar granule cells derived from both the WT and Pfizer KO mice (Sanchez-Nogueiro *et al.*, 2005). The identification of P2X7K receptors and its expression in the spleen explains some of these findings with the Glaxo KO mice (Nicke *et al.*, 2009).

In this study we have analysed the mouse genome for additional splice variants, and here we describe the expression and functional properties of two novel transcript forms with alternative exons 13, which encode shorter C-termini than the original exon 13. These C-terminal isoforms are predicted to escape inactivation in the Pfizer KO mouse strain. Given the importance of these mice to investigate the role of P2X7 receptors in health and disease, and the underlying assumption that they are null for functional P2X7 receptors, we have analysed the expression of these variants in the WT and the KO mice and the functional properties of the recombinant receptors expressed in HEK293 cells. We also identified a novel ΔC hybrid transcript expressed in the Pfizer KO mice.

Methods

Antibodies (Abs) and reagents

All reagents were purchased from Sigma Chemical Co. Ltd (UK) unless otherwise stated. A polyclonal rabbit Ab against the recombinant cytoplasmic C-terminal tail of mouse P2X7 receptors, residues 363–595, was obtained from Synaptic

Systems (Goettingen, Germany). The Alomone (Jerusalem, Israel) polyclonal rabbit Abs were raised against an antigenic epitope, KIRKEFPKTQGQYSGFKYPY, corresponding to residues 576–595 of rat P2X7 receptors (18/20 residues identical in mouse sequence) and against an extracellular domain epitope, KKGWMDPQSKGIQTGRC, corresponding to residues 136–152 of the mouse P2X7 receptor. Anti-hemagglutinin (HA) mouse monoclonal Ab was obtained from Covance (Princeton, NJ, USA). Anti-mouse and anti-rabbit horseradish peroxidase-conjugated secondary Abs were obtained from ThermoScientific (Loughborough, UK) and Bio-Rad (Hemel Hempstead, UK), respectively.

Culture media were supplied by Gibco (Life Technologies Ltd., Paisley, UK). Endoglycosidase H (EndoH) and N-glycosidase F kits were purchased from Roche (Welwyn Garden City, UK) and New England Biolabs (Hitchin, UK), respectively, and used according to manufacturers' instructions. The cross-linker, disuccinimidyl suberate (DSS) was supplied by Pierce (Thermo Fisher Scientific, Northumberland,UK). SDS and native gradient gels were purchased from Invitrogen (Life Technologies Ltd.).

Animals

All animal care and experimental procedures were performed with permission of the local Animal Health and Welfare Committees and in accordance with the UK Home Office guidelines. Adult C57 control and P2X7 KO: Pfizer (Solle *et al.*, 2001) and Glaxo (Sikora *et al.*, 1999) mice were used between the ages of 4 and 5 months. Animals were maintained in a 12 h light/dark cycle and fed normal diet and water *ad libitum*.

Reverse transcription (RT)-PCR analysis

Total cellular RNA was extracted from using RNA Isolation System (Promega, Southampton, UK) and equivalent amounts of RNA (5 μg) were reverse transcribed using random hexamers and Superscript first strand synthesis system for RT-PCR (Invitrogen). Reverse transcriptase was omitted in negative controls. RT-PCR was performed with primer sets specific for the various P2X7 receptor transcripts (see below). Cycling conditions were 94°C for 4 min, followed by 35 cycles of 94°C for 60 s, 58–65°C for 60 s, 72°C for 60 s with a final extension step of 72°C for 7 min. GAPDH expression levels were established in serial dilutions and at a lower number of cycles (22–25) to ensure that all the amplifications were carried out within the linear range to account for potential variations in RNA amounts, RT efficacy, etc., between different tissues tested. The PCR products were resolved by electrophoresis in 2% agarose gels and visualized by ethidium bromide staining. The identity of the PCR products was confirmed by sequencing and/or restriction analysis.

Rapid amplification of cDNA ends

3′ Rapid Amplification of cDNA Ends (3′-RACE) was performed using the FirstChoice® RLM-RACE kit (Ambion, Warrington, UK). Pfizer P2X7R KO total brain RNA (2 μL) was reverse transcribed in a 20 μL reaction volume containing 0.5 mM deoxynucleotide triphosphates (dNTPs), 10 units of RNase inhibitor, 100 units of M-MLV reverse transcriptase and 0.03 μg·μL^{-1} of 3′-RACE adapter primer: 5′-GCGAGCACAGAA TTAATACGACTCACTATAGGT12VN-3′ (all Ambion) at 42°C for 1 h. The negative control was generated from the same sample by omitting M-MLV reverse transcriptase. Thereafter, 1 μL of each cDNA was amplified in a 25 μL reaction volume using 400 nM P2X7 specific forward primer (see below) and 3′-RACE Outer Primer (Ambion). The cycling conditions were 35 cycles of 94°C for 30 s, 60°C for 30 s and 72°C for 3 min, and then followed by the final extension step of 72°C for 10 min. Second-step nested PCR was subsequently carried out using 2 μL of the outer 3′-RACE PCR product with 400 nM of mEx9Fv and 400 nM of 3′-RACE Inner Primer (Ambion).

PCR Primers:

mX7-j-Fv: 5′-TGCTCTTCTGACCGGCGTTG-3′ specific to exon 5

mEx9-Fv: 5′-GAGAACAATGTGGAAAAGCGG-3′ to exon 9

mEx11-Rev: 5′-CTGGAGTATGTGTTGATGAGCAAGTCA-3′ to exon 11

X713a-Rev: 5′-TCAGTAGGGATACTTGAAGCC-3′ variant 1 or exon 13a

X713b-Rev: 5′-TCTGTGAGAAACAAGTATCTAGGTTGG-3′ variant 3 or exon 13b

X713c-Rev: 5′-TCAGGTGCGCATACATACATG-3′ variant 2 or exon 13c

X7hyb-Rev: 5′-CCAAGTTCTAATTCCATCAGAAGCTG-3′

3′-RACE Adapter Outer Primer: 5′-GCGAGCACAGAATT AATACGACT-3′

3′-RACE Inner Primer: 5′-CGCGGATCCGAATTAATACGA CTCACTATAGG-3′

GAPDH primers: Fv: 5′-TCCACCCATGGCAAATTCCATG-3′ and Rev: 5′-TGGACTCCACGACGTACTCAGC-3′

Amplification of full length mRNAs

PCR was carried out in a 50 μL reaction in 1X Pyrococcus furiosus (Pfu) buffer [20 mM Tris-HCl (pH 8.8 at 25°C), 10 mM KCl, 10 mM (NH4)2SO4, 2 mM MgSO4, 0.1% Triton® X-100, 0.1 mg·mL–1 nuclease-free BSA] with 200 μM dNTPs, 1 unit Pfu polymerase (Promega), 0.4 mM primers and 1–3 μL DNA. The PCR cycling conditions were: 95°C for 2 min followed by 35 cycles of 95°C for 45 s, 58°C for 45 s, 72°C for 2 min, then 72°C for 10 min.

All PCR products were cloned directly into pGEM-T easy vector (Promega), clones analysed by restriction analysis and sequenced. When high-fidelity Pfu polymerase was used to obtain the full-length clones the T-A cloning was facilitated by 10 min incubation of the PCR product with ATP and Taq polymerase (Promega) at 70°C. For expression of recombinant receptors in HEK293 cells, cDNAs were subcloned into the Clonetech GFP-N1 vector using the Not I site to excise the coding sequence for GFP (Guo *et al.*, 2007).

Blue native PAGE

Fresh tissues from WT and P2X7$^{-/-}$ mice were disrupted by pushing through a 70 μm cell strainer in ice-cold PBS plus protease inhibitors, followed by centrifugation for 5 min at 200× *g*. The pellet was resuspended in hypotonic buffer (10 mM Tris-HCl pH 8, 2 mM EDTA, 1 mM PMSF and protease inhibitors cocktail (Roche) and left on ice for 20 min. When processing HEK293 cells expressing the P2X7 receptor variants, cells were washed three times with ice-cold PBS plus protease inhibitor, harvested and lysed in hypotonic buffer for 20 min. In both cases, cells were further disrupted by

repeated passes through 23G and 27G needles. The homogenate was centrifuged at 400× *g* for 10 min at 4°C to remove nuclei and then at 50 000× *g* for 35 min at 4°C. The pellet was resuspended in blue native (BN) sample buffer (Invitrogen) and solubilized with either 1% or 2% digitonin for 1 h on ice. For partial denaturation, samples were subsequently incubated with indicated concentrations of SDS at 37°C for 1 h. Solubilized membrane fractions were supplemented with 5% G250 additive buffer and centrifuged at 15 000× *g* for 10 min at 4°C. Samples were run on 4–16% native Bis-Tris gels, transferred onto PVDF membranes and immunoblotted with appropriate Abs.

Cross-linking receptors

For mouse tissue samples, a membrane preparation was carried out as described above for the BN-PAGE, and the pellet was resuspended and solubilized in BN sample buffer with 1% digitonin. For HEK293 cells, after washing with ice-cold PBS and harvesting in 1% Triton in PBS plus protease inhibitor (Roche), the samples were sonicated, incubated on ice for 30 min, and lysates were cleared by centrifugation at 15 000× *g* for 15 min at 4°C. DSS is a membrane permeable cross linker (ThermoScientific, Pierce) and was freshly prepared in DMSO, diluted to a final concentration of 4 mM and added to the protein samples at room temperature for 30 min. The reaction was quenched by the addition of Tris-HCl pH 7.5 to a final concentration of 50 mM for 15 min at room temperature. All samples were diluted in 2 × Laemmli buffer and analysed by 4–12% gradient SDS-PAGE and Western blotting.

Cell culture

HEK293 cells were maintained as described previously (Guo *et al.*, 2007; Moore and MacKenzie, 2007) and were routinely transfected using calcium phosphate or lipofectamine 2000 as described previously (Guo *et al.*, 2007).

Generation of stable cell lines

HEK293 cells were seeded in six-well plates and 12–16 h later, 60–70% confluent cells were transfected with the plasmid encoding the protein of interest using calcium phosphate. After 48 h post-transfection, geneticin (G418), 0.8 mg·mL^{-1} in fresh medium, was added to the cells to select for transfected clones. The medium was changed every other day to remove dead cells and replenish nutrients and antibiotics. Once confluent, cells were transferred into flasks and maintained in medium containing G418 (0.8 mg·mL^{-1}) for a total of 4 weeks from the transfection date. Cells were assayed for expression of the protein of interest via Ab detection using immunocytochemistry and Western blotting.

EndoH and N-glycosidase F treatments

Transfected cells were washed twice with PBS and collected in TEB buffer (50 mM Tris-HCl, 150 mM NaCl, 1% Nonidet P-40, 0.5% sodium deoxycholate, 0.1% SDS (Bio-Rad), pH 8). The lysate was sonicated, incubated on ice for 30 min, then centrifuged at 15 000× *g* for 15 min at 4°C to pellet unsolubilized material. The total protein content of the supernatant was then determined using the BCA™ Protein Assay Kit (ThermoSientific, Pierce) according to the manufacturer's instructions. For EndoH treatment, a volume equivalent to 20 µg protein was taken and made up to 16.2 µL with distilled water. 1.8 µL of 10× glycoprotein denature buffer was then added and the sample heated at 100°C for 10 min. 2 µL of 10× G5 Buffer was added, then 1 µL Endo H before incubating the samples at 37°C for 2 h. The reaction was terminated by the addition of one volume of 2× Laemmli buffer. For N-glycosidase F treatment, a volume equivalent to 20 µg protein was taken and made up to 9 µL with distilled water. 1 µL of 10× glycoprotein denature buffer was then added to all tubes and the samples boiled at 100°C for 10 min. Two microlitres 10× G7 reaction buffer, 2 µL of 10% NP40 and 5 µL distilled water were added to each sample. Following the addition of 1 µL PNGase F, tubes were incubated for 2 h at 37°C. The reaction was terminated by the addition of one volume of 2× Laemmli buffer. Samples were analysed by SDS-PAGE and Western blotting.

Biotinylation of surface receptors

Procedures were essentially conducted as described previously (Boumechache *et al.*, 2009). Briefly, cells were rinsed with ice cold Dulbecco's PBS (DPBS, -$CaCl_2$, -$MgCl_2$, Gibco, Paisley, UK) and incubated with freshly prepared Sulfo-NHS-SS biotin (ThermoScientific, Pierce), diluted in DPBS (1 mg·mL^{-1}), for 30 min at 12°C. Non-reactive biotin was quenched with 50 mM glycine, followed by three washes with cold DPBS. The cells were subsequently lysed in 150 µL TEB and sonicated. The resultant lysate was cleared by centrifugation at 15 000× *g* for 15 min at 4°C and 50 µL of the supernatant was diluted in Laemmli buffer and used to determine total protein levels. The biotinylated proteins in the remaining 100 µL were precipitated by incubation with 30 µL of streptavidin beads (Pierce) on a rotating wheel at 4°C for 2 h. After three washes in TEB, proteins bound to streptavidin beads were eluted in sample buffer (20 µM dithiothreitol in Laemmli buffer) and subjected to SDS-PAGE and immunoblot analysis. Restriction of biotin labelling to surface receptors was confirmed by lack of reactivity to β-actin.

Co-immunoprecipitation

Transfected cells were washed twice in ice-cold HEPES buffered saline supplemented with 2 mM EDTA, harvested and lysed in hypotonic buffer. The lysate was homogenized by 10–20 passages through each of a 23G and a 27G needle. Membranes were pelleted at 15 000× *g* for 15 min at 4°C then solubilized in 1% n-dodecyl-β-maltoside (DDM) solution for 1 h at 4°C. The samples were ultracentrifuged at 50 000× *g* for 1 h and the supernatant then pre-cleared using protein G beads (Pierce) for 30 min to remove proteins binding non-specifically to the beads and the agarose. Mouse monoclonal anti-HA Ab (5 µg) was added to the sample, incubated at 4°C for 3 h followed by addition of 70 µL of protein G beads for a further 1 h. Protein : Ab : bead complexes were pelleted by centrifugation, washed three times in 1 mL 1% DDM solution and resuspended in 40 µL 2× Laemmli buffer before analysis by SDS-PAGE and Western blotting.

Electrophysiology

Whole cell patch clamp recordings were made at room temperature using an Axopatch 200A amplifier (Axon Instruments, CA, USA) as described previously (Guo *et al.*, 2007). Patch pipettes (4–6 mΩ) were pulled from thick-walled boro-

silicate glass (1B150F-4, World Precision Instruments, Inc., Hitchin, UK) and back-filled with intracellular solution (151 mM CsCl, 10 mM HEPES, 10 mM EGTA, 3 mM MgCl) and mounted on a CV201 head stage. Cells were maintained in normal extracellular solution contained as follows: 140 mM NaCl, 5 mM KCl, 2 mM $CaCl_2$, 1 mM $MgCl_2$, 10 mM D-glucose, 10 mM HEPES, pH 7.3. The voltage was held at –60 mV and the agonist, 2′(3′)-*O*-(4-benzoylbenzoyl)-ATP (BzATP), was applied directly to the cell using a picosprizer to ensure rapid solution exchange in the immediate vicinity of the cell. To generate concentration-response relationships, two to three short (5 s) applications of 1 mM BzATP were made, separated by a 2 min wash period. Once the response had stabilized, other concentrations were then applied at least twice. Peak current amplitudes were then normalized either to the 1 mM response or to the capacitance of the cell. The data was acquired using HEKA PulseMaster software (HEKA Instruments Inc.,Bellmore, NY, USA) and exported to Igor Pro for analysis.

Data analysis

Graphs were generated using Excel software (Microsoft, Mountain View, CA, USA) and statistical analysis was performed using unpaired *t*-test using GraphPad software (La Jolla, CA, USA).

Computational analysis of structural features in the C-terminus of P2X7 receptors

We employed the algorithm DISOPRED (http://bioinf.cs.ucl.ac.uk/disopred/) for the prediction of protein-disordered regions in P2X7 variants. Disordered regions within polypeptides are often characterized by a low-sequence complexity, a compositional bias towards aromatic and hydrophilic residues and predicted high flexibility. The DISOPRED algorithm was trained on a set of 750 non-redundant sequences for which electron density is missing in the corresponding high-resolution X-ray structure, indicating disorder and flexibility (Ward *et al.*, 2004).

For the prediction of protein-binding regions within the disordered stretch identified in the P2X7 variants we employed the algorithm ANCOR (http://anchor.enzim.hu/). This algorithm identifies segments within disordered regions that cannot form favourable intrachain interactions as to fold on their own, and which are likely to adopt conformations with more favourable energy by interacting with a globular protein partner (Dosztanyi *et al.*, 2009; Meszaros *et al.*, 2009).

Results

Identification of mP2X7 ΔC splice variant mRNAs

The full-length P2X7 receptor is encoded by 13 exons with the canonical exon 13 encoding the long C-terminus specific to this subunit. Analysis of mouse sequence databases identified two more variants of P2X7 transcript. Variant 3 (sequence NM_001038839 and supported by expressed sequence tags (ESTs): AK089434, AK144585, BB810482, BY544874, BY548370, BY764453) contains 13 exons but with a unique very short exon13b, that encodes just one residue before the stop codon. Variant 2 (sequence NM_001038845 and supported by ESTs: AK171132, BY533776, BY537985) also consists of 13 exons but contains yet another short exon 13 (13c) (Figure 1A). These two alternative exons 13 encode much shorter C-termini than the original exon 13a. Variant 2 (13b) would translate into a receptor that is truncated at position 430, and 13c would have an alternative C-terminus with specific 11 amino acids beyond the common residue 430 (Figure 1B).

Tissue expression of mP2X7 receptor ΔC variants

In order to understand whether or not these truncated variants contribute to P2X7 receptor diversity, we initially analysed their expression in various WT and $P2X7^{-/-}$ mouse tissues. RT-PCR with specific sets of primers identified the 13a splice variant to be the predominant form in all WT tissues tested. The 13b splice variant was also detected in all tissues with strongest expression in the brain, salivary gland (SG) and spleen while the 13c variant was present in the brain, with lower level expression in lung and SG (Figure 2). Using specific sets of primers, we were able to amplify the full-length mRNAs of 13b and 13c transcripts.

Corresponding analysis performed in tissues from the Glaxo $P2X7^{-/-}$ mice demonstrated that the 13a variant is the predominant form there; no significant expression of 13b and 13c variants was detected in any of the tissues tested (Figure 2B). The exon 13a-containing variant was previously identified in the Glaxo KO mice: it corresponds to P2X7k, which uses a novel exon 1, downstream from the disrupted exon 1a (Nicke *et al.*, 2009). It appears therefore that transcripts containing this novel exon 1 favour the exon 13a. In agreement with this, amplifications with primers for exon 1a or 1k, combined with primers for 13a, 13b or 13c resulted in full-length transcripts where exon 1a coexisted with all three alternative exons13, but exon 1k was detected only in combination with 13a (Figure 2E).

As expected, in the Pfizer KO tissues, there was no expression of the deleted exon 13a but there was low expression of 13b in brain, SG and spleen (Figure 2C). Surprisingly, further amplification using primers to exons 9 to 11 detected significant expression in all Pfizer KO tissues tested (Figure 2D). This suggested the existence of yet another 3′ transcript variant. To identify this mRNA, we used 3′-RACE PCR with Pfizer KO brain cDNA as a template. Following cloning and sequencing of the resulting amplicons, we identified a hybrid transcript containing sequences of P2X7 mRNA upstream of exon 12, part of exon 13 followed in-frame by the sequence of the targeting vector used to disrupt the P2X7 gene. This transcript was clearly polyadenylated as it was identified using an oligo-dT RACE primer. If translated, such hybrid mRNA would encode a P2X7 receptor with a truncated and altered C-terminus containing 75 aa encoded by the WT exon 13a followed by another 22 aa with no clear sequence homology (Figure 1C). RT-PCR using a primer for exon 9 combined with a primer specific for the hybrid sequence showed strong expression of the hybrid transcript in brain, spleen and SG of the Pfizer KO mice (Supporting Information Figure S1). Furthermore amplification using a set of primers incorporating the ATG start codon of the WT P2X7 receptor and the novel stop codon amplified the full-length hybrid transcript, which further suggests that it is a stable mRNA.

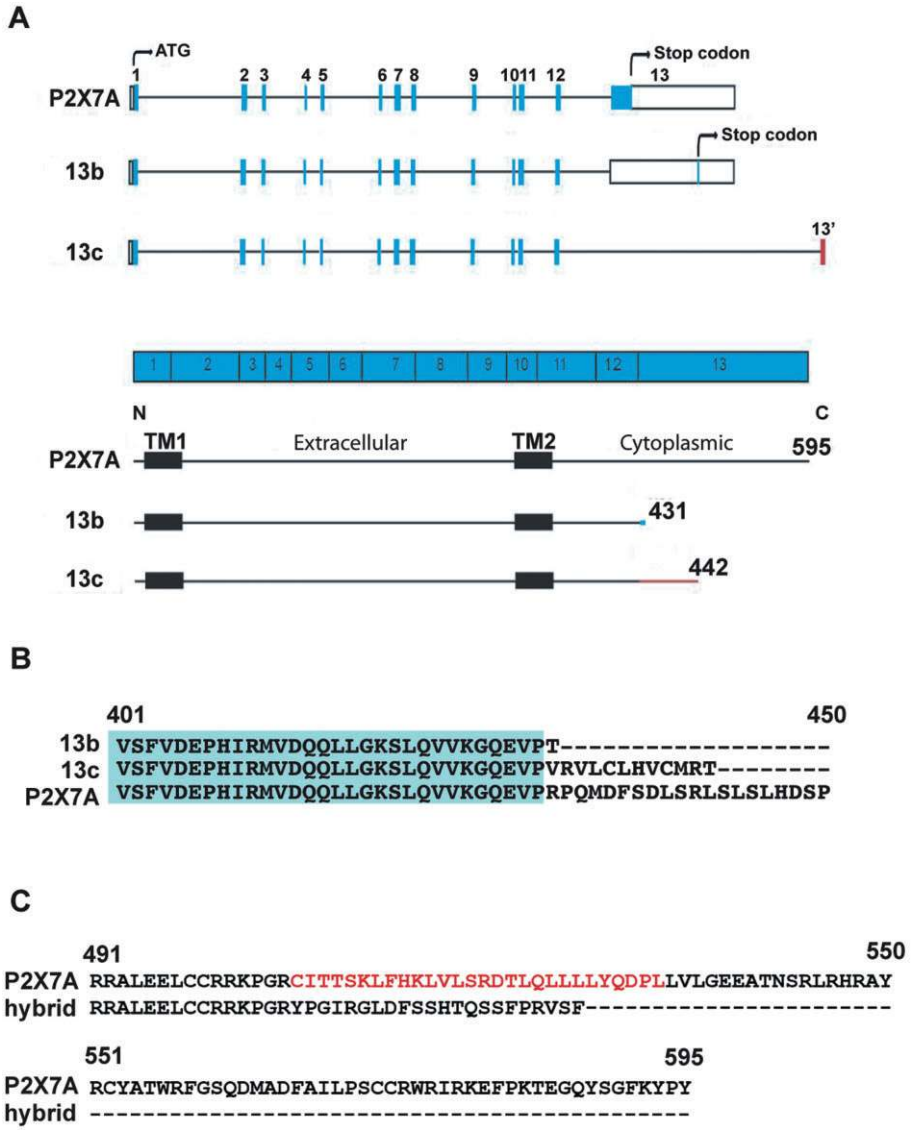

Figure 1

Alignment and genomic organisation of mouse P2X7 receptor variants. (A) The genomic organization of the alternative mouse 13 exons. (B) Alignment of predicted protein sequences of the alternative P2X7 C-termini resulting from translations of the 3'-variants. (C) Alignment of predicted protein sequence of the C-termini of the hybrid P2X7 and P2X7A receptors. The region encoded by the exon sequence used for targeting in the Pfizer KO is shown in red.

Blue native PAGE analysis of P2X7 receptors shows expression of trimeric complexes in WT and P2X7$^{-/-}$ mice tissue

Having shown expression of the 13B transcript in brain, spleen and SG of WT mice and, to a lesser extent, also in Pfizer KO mice, combined with high levels of expression of the hybrid transcript in the Pfizer tissues, we analysed levels of protein expression. Extracts from WT and the two P2X7$^{-/-}$ strains were probed using P2X7 receptor Abs raised to different regions of the receptor; the distal C-terminus (C-term), the extracellular domain (EC) and the entire C-terminus (SySy). Proteins were analysed in their native state following solubilization in digitonin and then with low concentrations of SDS added to cause partial dissociation of the complex to resolve the different multimeric states. Using the C-term Ab, a band running at ~440 kDa was detected with greater intensity in WT brain samples than in either of the KO strains and in the presence of 0.1% SDS, this dissociated to give three bands of mass corresponding to monomer, dimer and trimer (Figure 3A). There was an additional band at ~200 kDa present at similar intensity in WT and KO samples and also seen in the presence of 0.1% SDS, and this probably represents non-specific binding of the Ab. The EC domain Ab similarly detected a band at 440 kDa in the WT brain samples not seen in the KO samples, which dissociated to give monomer, dimer and trimer of the same size as detected with the C-term Ab

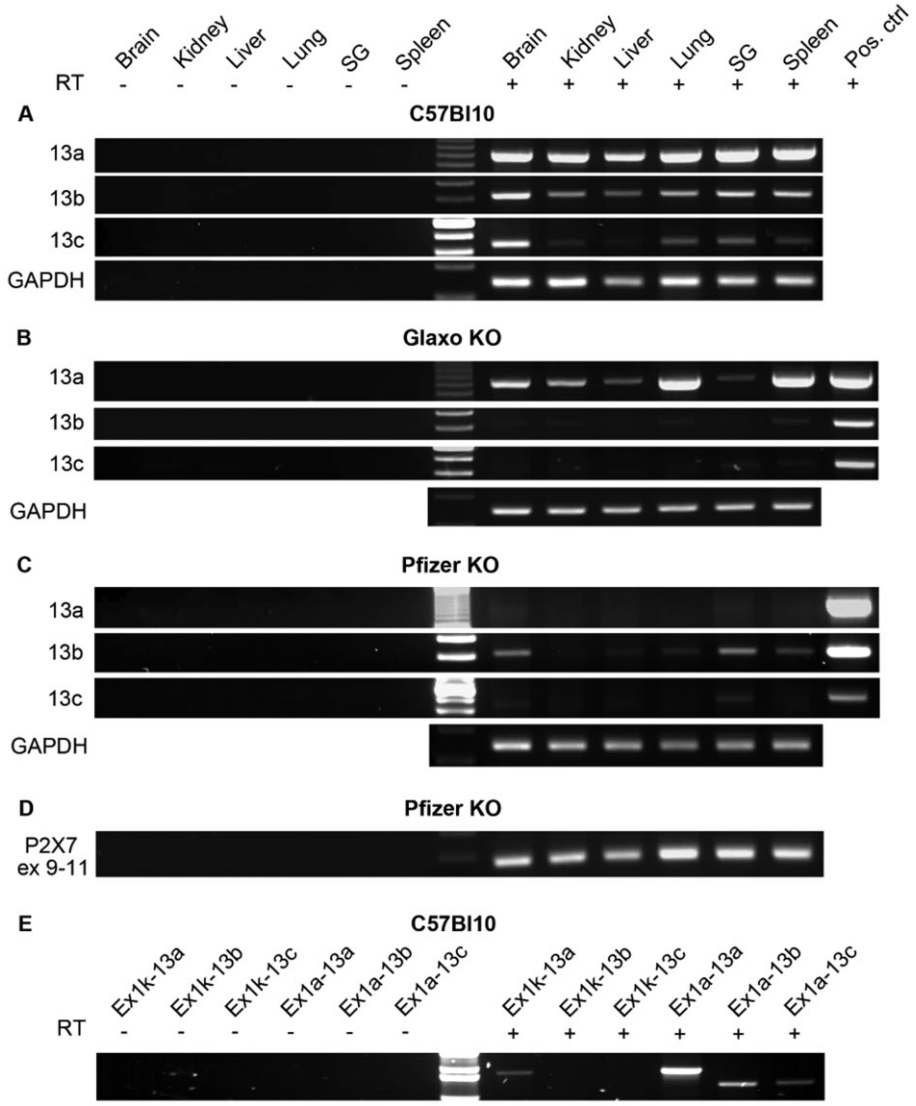

Figure 2

RT-PCR analysis of the tissue expression of ΔC variants of the mP2X7 receptor. Representative examples of gel analysis of PCR products are shown. Primer sets specific for exons 13a, 13b and 13c were used to identify these transcripts in tissues from the WT (A), Glaxo (B) and Pfizer (C) P2X7$^{-/-}$ mice. (D) Amplifications between exons 9 and 11 of the hybrid transcript in Pfizer KO tissues. (E) Amplification of the full-length spliced variants in WT brain tissue shows a correlation between the 5′- and 3′-end P2X7 splicing events with transcripts containing the novel exon 1k only occurring with exon 13a, whereas exon 1a occurs with all three exons 13. (–RT) denotes the negative controls, where reverse transcriptase was omitted during preparation of the first strand and (+Pos. Ctrl) in B and C represent positive control amplifications using WT cDNAs. GAPDH panels are positive controls for equivalent loading.

(Figure 3B). Thus, we are confident that this represents the full-length P2X7 receptor. There was no band at ~200 kDa but instead a high molecular weight smear in all the brain samples. There was no evidence of bands that might correspond to truncated P2X7 receptor subunits in any of the brain samples, even though this Ab should detect the 13B/C and hybrid variants. In spleen, the EC Ab detected a band at 440 kDa in WT and Glaxo KO samples but not in the Pifzer KO mice samples, and this dissociated in the presence of either 0.1% SDS (WT) or 0.2% SDS (Glaxo) to give bands corresponding to monomer, dimer and trimer of the full length P2X7A/K variants (Figure 3C). The Pfizer KO spleen samples also gave three bands in the presence of SDS, but running at lower molecular mass than the bands detected in the samples from the other strain of mice, consistent with the detection of a truncated P2X7 receptor splice variant. The results were similar in SG; for the Pfizer samples, in the presence of SDS, there was evidence of a truncated P2X7 splice variant (Figure 3D). The Glaxo SG samples did not show bands corresponding to the full length P2X7K receptor which is consistent our earlier report that the P2X7K receptor was expressed predominantly in the spleen (Nicke *et al.*, 2009). In the absence of SDS, the Pfizer spleen and SG samples gave a high molecular weight

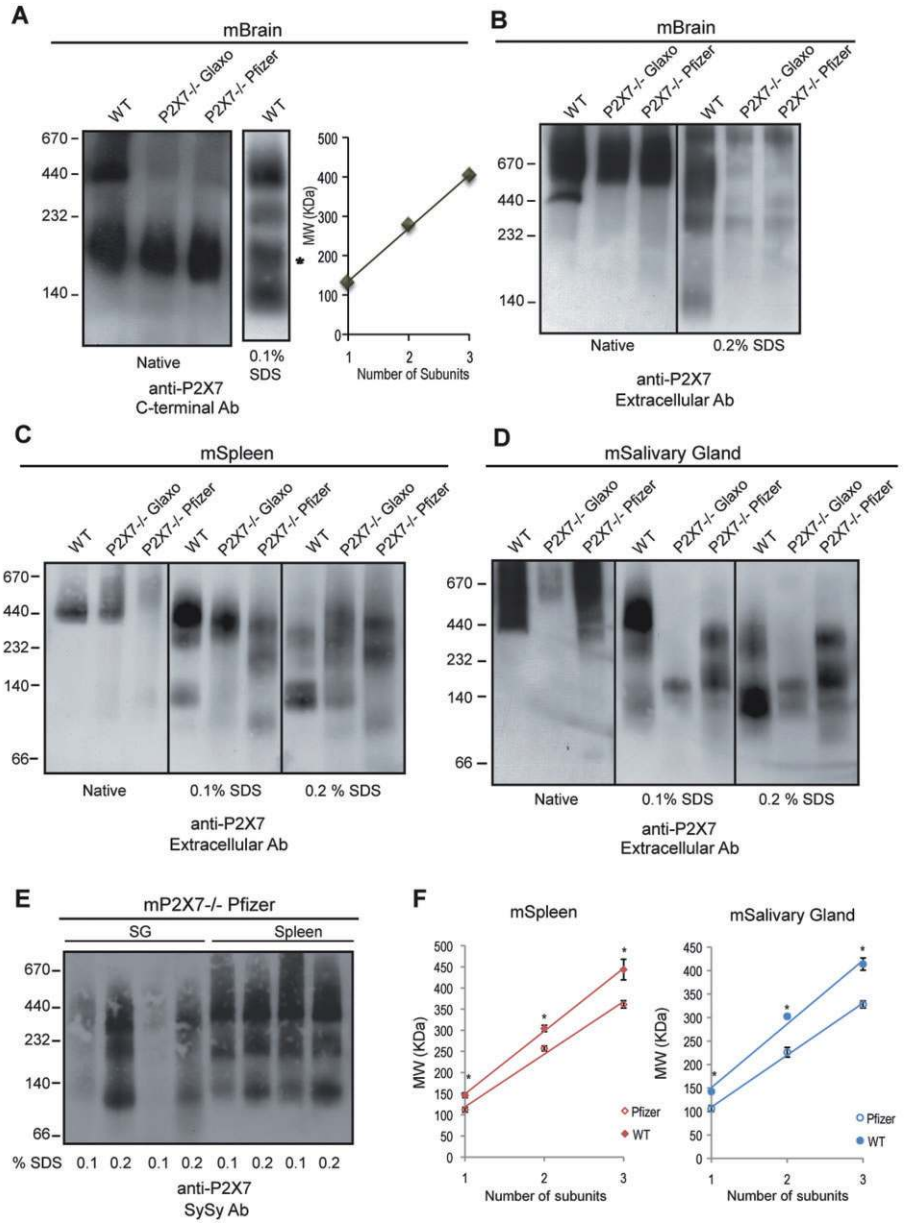

Figure 3

Analysis of P2X7 complexes in WT and P2X7$^{-/-}$ mice. (A–E) membrane preparations from WT and P2X7$^{-/-}$ tissues were solubilized in 1–2% digitonin, incubated with or without 0.1-0.2 % SDS to partially denature the complexes, then analysed by BN-PAGE, and finally immunoblotted with anti-P2X7 receptor Abs directed against the distal C-terminal domain (A) the extracellular domain of the protein (B–D) or proximal C-terminus (E). (F) Plots of molecular mass versus subunit number show the difference between the sizes of the trimer (T), dimer (D) and monomer (M) species (kDa) detected for WT (in kDa, T: 444 ± 24; D: 304 ± 7; M: 146 ± 6 and T: 414 ± 13; D: 303 ± 5; M: 143 ± 1 for spleen and salivary gland respectively) and P2X7$^{-/-}$ (Pfizer) (T: 361 ± 8; D: 257 ± 6; M: 112 ± 6 and T: 328 ± 7; D: 226 ± 10; M: 106 ± 6 for spleen and salivary gland respectively) tissues. Data are mean ± SEM of 4–5 animals; *$P < 0.005$.

smear but there was no clear band of a size expected for a homotrimer of one of the ΔC variants, suggesting that these variants could have a tendency to aggregate.

We analysed further spleen and SG samples from the Pfizer KO mice, using either 0.1 or 0.2% SDS to cause partial disassembly and probed with the SySy Ab. Again, bands of molecular mass consistent with trimers, dimers and monomers were detected in the presence of 0.2% SDS, and their recognition by a second P2X7 receptor Ab raised to a different region of the receptor is further evidence that we were detecting truncated P2X7 receptor variants. It is unclear why bands with 0.1% SDS for the SG samples were so poorly resolved. Western blot of the recombinant P2X7 receptor variants showed that both Abs were capable of detecting the 13B and hybrid variants in addition to P2X7A (Supporting Information Figure S2). Analysis of molecular mass for WT and Pfizer SG and spleen samples

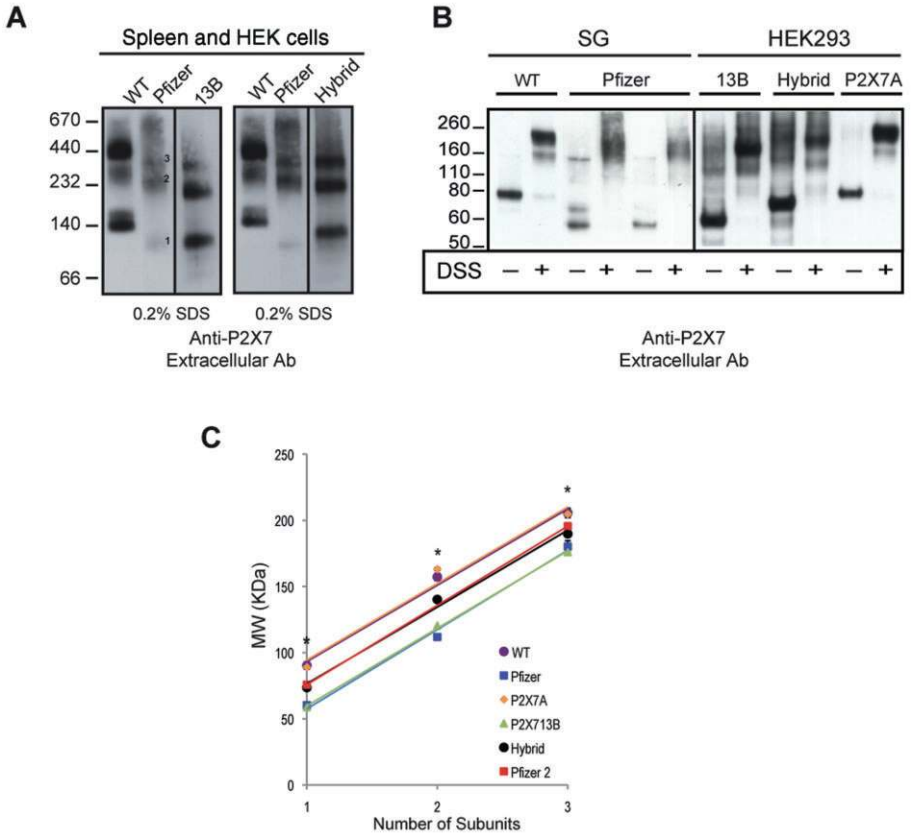

Figure 4

Size correlation of P2X7 immunoreactive species in Pfizer P2X7$^{-/-}$ mice with recombinant truncated P2X7 receptor variants. (A) Membrane preparations from WT and Pfizer P2X7$^{-/-}$ spleen and HEK293 cells expressing recombinant P2X713B or hybrid were solubilized in 1% digitonin, incubated with 0.2 % SDS to partially denature the complexes, then analysed by BN-PAGE and immunoblotted with the extracellular domain (EC) Ab. (B) Immunoblot analysis of membrane extracts from SG of WT and P2X7$^{-/-}$ (Pfizer) mice and HEK293 cells overexpressing P2X7A, 13B or hybrid using the EC Ab. After solubilization, samples were treated with or without the cross-linker DSS prior to separation by SDS-PAGE. (C) Plot of molecular mass versus subunit number shows that the size of the species found in SG from P2X7$^{-/-}$ (Pfizer) mice are similar to those detected for the recombinant expression of the 13B and hybrid variants, where Pfizer represents bands corresponding to 13B (Monomer: 59 ± 2 kDa; Trimer: 182 ± 4 kDa), and Pfizer 2 represents the bands corresponding to hybrid (M: 74 ± 2 kDa; T: 196 ± 9 kDa). Pfizer SG species differed significantly in mass from WT mice (M: 90 ± 2 kDa; T: 205 ± 3 kDa). Data are mean ± SEM of 3–6 animals; *$P < 0.005$.

with Student's *t*-test indicates that the bands in the Pfizer samples are significantly different in size from those in WT tissue ($n = 3$–6, $P < 0.005$) (Figure 3F). Additionally, there was a small difference in mobility between dimer and trimer bands detected in Pfizer spleen compared with SG, suggesting that there might be more expression of the hybrid in the spleen and the 13B variant in SG. In some Pfizer spleen samples (Figure 3E) there was an indication of a doublet for the middle band, again suggesting the expression of both hybrid and 13B dimers.

A comparison of P2X7 receptor immunoreactive complexes in SG and spleen of KO mice (Pfizer) and the recombinant P2X7 truncated variants

We compared the sizes of P2X7 receptor immunoreactive species from Pfizer KO mice with the recombinant P2X7 variants using BN-PAGE and also cross-linking proteins prior to separation by SDS-PAGE (Figure 4). The blot in Figure 4A shows WT and Pfizer spleen samples from two different mice compared with either the 13B variant or with the hybrid P2X7 receptor. The recombinant truncated variants expressed in HEK293 cells are clearly capable of assembling to form trimers. The bands corresponding to dimer and trimer in the Pfizer spleen samples correspond more closely to the hybrid variant but there is a monomeric band of mass closer to the 13B variant. In some samples, we also resolved a higher molecular mass band probably corresponding to a hexamer (dimer of trimers) as has previously been reported for P2X receptors (Antonio *et al.*, 2011). Using SDS-PAGE we compared SG samples with and without cross-linker with the recombinant proteins (Figure 4B). SG samples from two different mice are shown, and a monomer similar in size to the 13B variant (~60 kDa) is evident in both, with a higher band of similar size to the hybrid (~70 kDa) also clearly evident in one of the samples. This higher band was detected in SG from two other animals also. In the presence of DSS, a higher

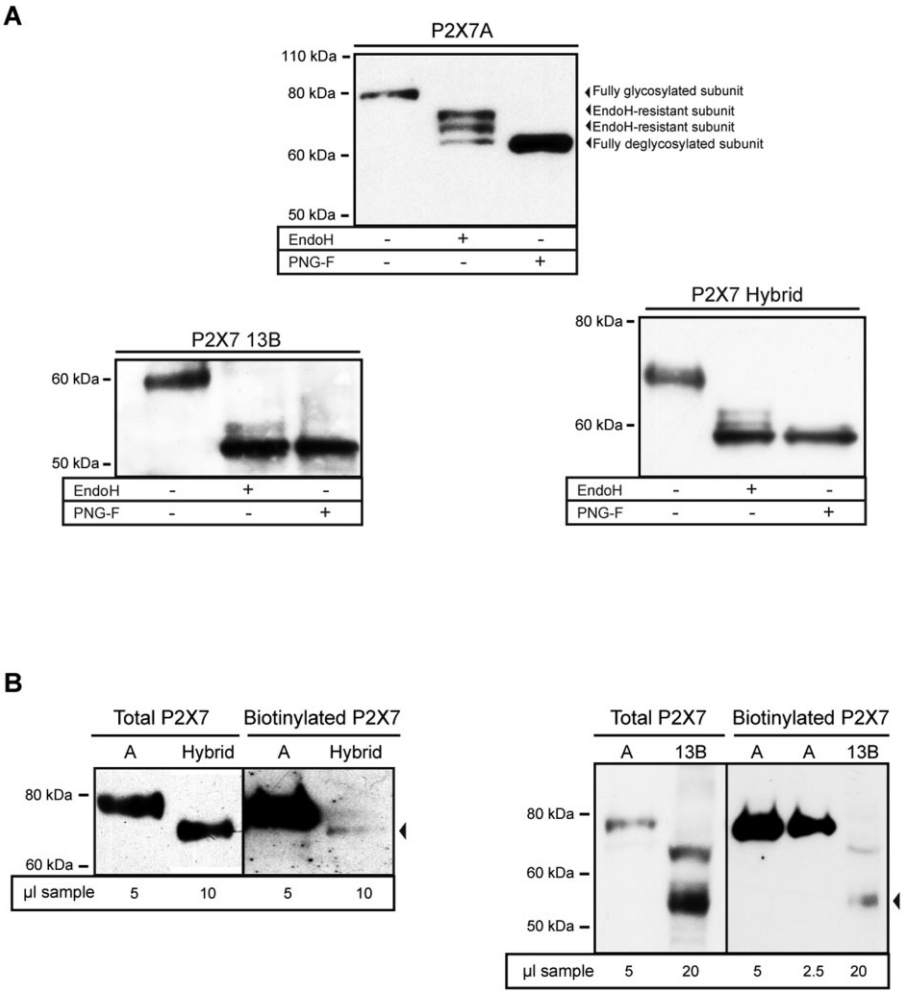

Figure 5

Inefficient trafficking of the P2X7 receptor ΔC variants to the plasma membrane. (A) Western blot analysis of protein samples subjected to deglycosylation treatments (with N-glycosidase F (PNG-F) or EndoH) shows that the majority of P2X7A protein is complex glycosylated and thus resistant to EndoH, whereas the majority of the 13B and hybrid protein is fully deglycosylated by EndoH. (B) Surface biotinylation followed by Western blot analysis shows that the proportion of receptors expressed at the plasma membrane is much higher for P2X7A, than for either the 13B splice variant or the hybrid construct. The arrow heads point to the very faint bands detected for the surface biotinylated 13B and hybrid variants.

molecular weight species was detected; there was generally some smearing and an indication of a doublet, consistent in size with 13B and hybrid trimers. Mean molecular masses for between 3–6 experiments are plotted in Figure 4C and confirm that the sizes of the bands correspond well to the recombinant 13B and hybrid monomers and trimers. The differences in molecular mass between Pfizer and WT SG bands are again significant ($P < 0.005$) for both monomers and trimers.

The P2X7 ΔC truncated variants are inefficiently trafficked to the plasma membrane

With the evidence of expression of the ΔC variants, we next wanted to investigate their functionality. The 13B and hybrid forms of P2X7 can form homotrimers. To measure the efficiency with which these traffic out of the endoplasmic reticulum (ER) to the trans-Golgi network (TGN) we compared the extent of complex glycosylation of truncated and full length P2X7 by the sensitivity of N-linked glycans to EndoH (Figure 5). For the full-length P2X7A receptor, the majority of the protein showed EndoH resistance and ran at a higher molecular mass than the sample treated with N-glycosidase F, indicating trafficking at least as far as the TGN (Figure 5A). In contrast, for the truncated 13B variant and the hybrid construct, the majority of the protein was EndoH-sensitive, suggesting it was retained in the ER. There were, however, faint bands at a higher molecular mass suggesting a small proportion did reach the TGN. Consistent with these findings, when we compared plasma membrane expression of these variants, by isolating surface biotinylated proteins, the levels of P2X7A were much higher than for 13B or hybrid P2X7 proteins, indicating

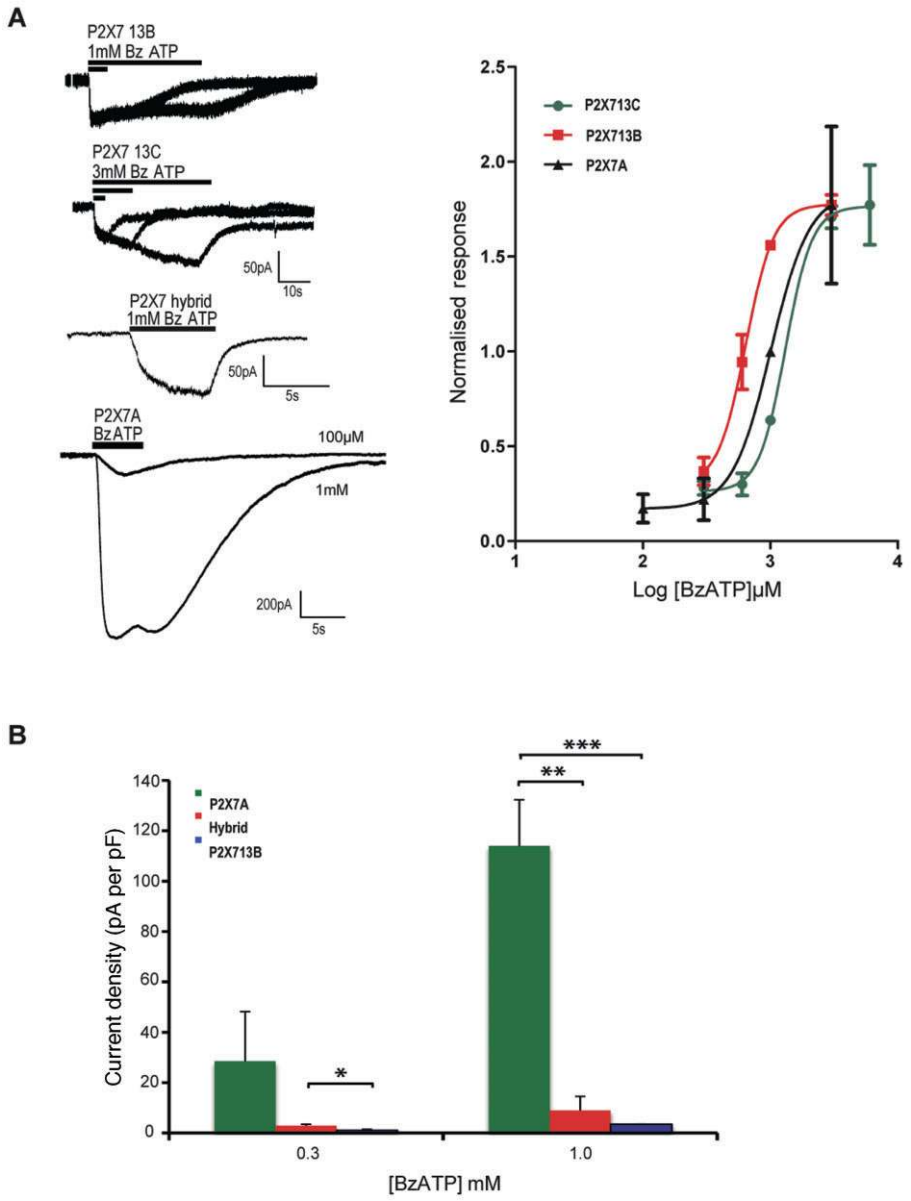

Figure 6

Whole-cell currents mediated via the P2X7 ΔC variants are of much lower amplitude than P2X7A receptor currents. (A) Whole cell currents activated by BzATP were measured at a holding potential of −60 mV in HEK293 cells expressing the different P2X7 receptor variants. To generate concentration-response relationships the peak current amplitudes were normalized to the response to 1 mM BzATP for each cell. The EC_{50} values were, 1.0 mM for P2X7A, 0.64 mM for P2X7 13B and 1.3 mM for P2X7 13C, indicating that there is no large shift in agonist potency. (B) Peak current amplitudes at different concentrations of BzATP were normalized to cell capacitance to calculate peak current densities for the P2X7A, 13B and hybrid variants.

that these truncated variants are predominantly intracellular (Figure 5B).

The P2X7 receptor ΔC variants are functional but mediated much smaller currents than the P2X7A variant

Patch clamp measurements were made to determine whether or not functional receptors reached the plasma membrane, albeit inefficiently (Figure 6). Following expression in HEK293 cells, BzATP-evoked inward currents were recorded for 13B, 13C and hybrid receptors. All currents measured were slowly desensitizing, as shown for the 13B and 13C responses to a 20 s application of agonist (Figure 6A). The normalized concentration-response relationships are shown for P2X7A receptors and the 13B and 13C variants, and EC_{50} values were 1.0 mM, 0.64 mM and 1.3 mM respectively. Currents for the 13B/C and hybrid variants were much smaller in amplitude than for P2X7A receptors, consistent with their low expression at the plasma membrane. Mean current den-

sities evoked by 0.3 mM and 1.0 mM BzATP for both 13B and the hybrid receptor were <10% of P2X7A receptors (Figure 6B). We also tested whether or not activation of either of the ΔC variants could increase membrane permeabilization to ethidium, similar to P2X7A receptors, but we did not observe any increase in ethidium uptake suggesting that either this function is lost, or that the surface expression of these receptors is too low (results not shown).

The P2X7 13B splice variant co-assembles with P2X7A receptors and acts in a dominant negative fashion

At the RNA level, the 13B splice variant is co-expressed with P2X7A in several of the WT mice tissues, in particular brain, SG and spleen. Our failure to detect expression of the 13B protein in WT tissue, indicates that expression is much lower than for P2X7A; however, even a low level of expression might functionally be relevant if there is an interaction between 13B and P2X7A. For example, for the human P2X7 receptor, the ΔC variant hP2X7B is reported to associate with and potentiate the responsiveness of hP2X7A when they are co-expressed (Adinolfi *et al.*, 2010). We therefore co-expressed P2X7A with the 13B splice variant to see if there was a structural or functional interaction between these two isoforms (Figure 7). The 13B variant, rather than potentiating the response to P2X7A, instead acted in a dominant negative way to suppress P2X7A receptor currents by ~70% (Figure 7B). This suggests that the two subunits might be capable of forming a heteromeric complex with the full-length subunit unable to rescue and restore trafficking of the truncated subunit. To look for further evidence of an interaction between these two variants, co-immunoprecipitation experiments were performed using the anti-HA Ab to pull down the HA-tagged 13B variant and blotting with the anti-C-terminal Ab to detect the full length P2X7A receptor (Figure 7C). Both variants were either transiently co-expressed or P2X7 13B was transiently expressed in HEK293 cell stably expressing P2X7A. In both cases the two subunits co-immunoprecipitated, consistent with the formation of a heteromeric complex between them.

The effects of co-expression on trafficking of the receptors to the plasma membrane were tested by isolating surface biotinylated proteins. We compared P2X7A co-expressed with enhanced green fluorescent protein (EGFP) with P2X7A co-expressed with 13B and then 13B alone (Figure 7D). Surface expression of P2X7 was reduced by about ~60% when co-expressed with 13B, and, surprisingly, so was its total expression. This is unlikely to be competition for synthesis because in the control, we substituted EGFP for 13B. We therefore think it more likely that this reflects a reduction in the stability of the heteromers compared with the homomers and an increase is the rate of degradation of these complexes. Total and surface expression of 13B was also reduced by co-expression with P2X7. The reduction in whole cell current can, therefore, be attributed, at least in part, to a reduction in the number of receptors at the plasma membrane.

Discussion

Similar to the human isoform of the P2X7 receptor, which has a prevalent ΔC splice variant (hP2X7B) in addition to the full-length hP2X7A variant, there are two ΔC splice variants of the mouse P2X7 receptor, and their expression and function has not previously been studied. These two variants are identical with P2X7A between residues 1–430, one of the variants then terminates at T431 (P2X7 13B), and the other has an additional 11 amino acids at the C-terminus (P2X7 13C). Because they utilize different final exons 13, the prediction is that their expression should not be disrupted in the Pfizer KO mice. We show expression of the RNA of these truncated variants in WT mice brain, SG and spleen. In addition, transcripts for the 13B splice variant and a novel ΔC hybrid variant, containing sequences of P2X7 upstream of exon 12, part of exon 13 followed in-frame by the sequence of the vector used to disrupt the P2X7 gene, were identified in tissue from Pfizer KO mice. Western blot analysis indicates the expression of trimeric P2X7 receptor complexes in the Pfizer KO mice spleen and SG with molecular mass consistent with the expression of a ΔC form of the receptor. Analysis of the recombinant variants expressed in HEK293 cells showed that although they form stable homotrimers, the efficiency with which they traffic out of the ER to reach the TGN and plasma membrane is considerably reduced compared with the full-length variant. Not surprisingly, the whole cell currents mediated by these receptors were of much reduced amplitude compared with P2X7A receptors. Also mP2X7 13B, when co-expressed with the full-length P2X7A receptor, acted in a dominant negative fashion to reduce the surface expression of P2X7A and the amplitude of agonist-evoked whole cell currents. Thus we conclude that the ΔC splice variants contribute to the diversity of P2X7 receptor-mediated responses and that the Pfizer KO mice, similar to our findings in the Glaxo KO mice, are not null for P2X7 receptor expression in all tissues.

Our failure to detect expression of protein corresponding to the ΔC forms of P2X7 in WT mouse tissue indicates that they are expressed at a much lower level than the full-length P2X7A receptor. This contrasts with the reportedly high expression of the hP2X7B, a ΔC splice variant (Cheewatrakoolpong *et al.*, 2005; Adinolfi *et al.*, 2010). Here though, expression was only reported at the level of mRNA, and the abundance of the hP2X7B protein remains unknown. The hP2X7B protein has a larger C-terminal deletion than the mouse ΔC variants; it retains an intron between exons 10 and 11, which causes insertion of a stop codon, and it is 231 amino acids shorter than the P2X7A protein. When the hP2X7B protein was expressed in HEK293 cells, calcium responses and membrane depolarization were less than that mediated by hP2X7A, but, surprisingly, it potentiated responses mediated by the P2X7A variant when the two variants were co-expressed (Adinolfi *et al.*, 2010). By surface biotinylation, we have compared the surface expression of the hP2X7A and hP2X7B variants in HEK293 cells and found that hP2X7B receptors, similar to mP2X7 13B, are very inefficiently trafficked to the plasma membrane (Supporting Information Figure S3). Despite this, its expression was shown to increase endoplasmic reticulum Ca^{2+} levels, NFATc1 activation and growth rates (Adinolfi *et al.*, 2010). Thus the low surface expression of the ΔC variants does not necessarily imply that functionally they do not have an important role to play. In addition there is the possibility that their expression could be

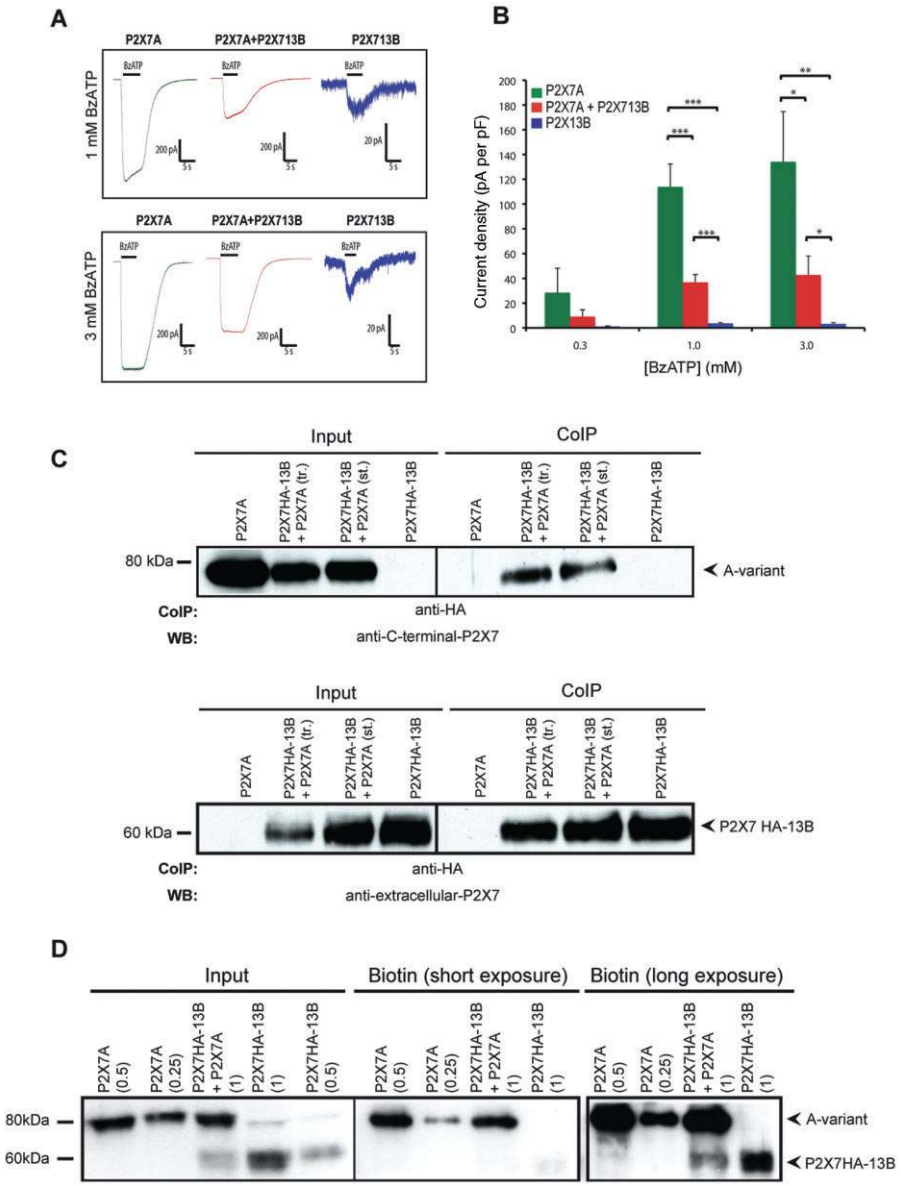

Figure 7

The P2X7 13B splice variant can interact with P2X7A receptors to inhibit their expression and function. (A) BzATP-evoked inward currents were recorded from HEK293 cells expressing P2X7A, the 13B splice variant or co-expressing these two variants. Cells were transiently transfected with cDNAs at a ratio of 2:1 (13B:P2X7A). The amount of each cDNA used in the single transfected cells was the same as for the co-transfected cells. The peak current amplitudes were normalized to cell capacitance to calculate current densities. The results show that the 13B splice variant mediates very small currents and inhibits the P2X7A response when the two variants are co-expressed. (C) The 13B splice variant tagged at the C-terminus with the HA epitope was co-expressed with P2X7A, either by transient co-transfection of both variants (tr) or by the transient transfection of the 13B variant into HEK293 cells stably expressing P2X7A (st). Following immunoprecipitation with anti-HA Ab, the blots were probed either with the anti-HA or anti-P2X7 C-terminal Ab, which is able to recognize P2X7A but not the 13B variant. The lower blot shows that P2X7A is co-immunoprecipitated with the 13B-HA splice variant, indicating a structural interaction between these two subunits. In the absence of the 13B splice variant, P2X7A was not detected following immunoprecipitation with anti-HA, as predicted. (D) Surface biotinylation followed by Western blot analysis shows that the proportion of P2X7A receptors expressed at the plasma membrane was reduced when co-expressed with the 13B splice variant. We compared P2X7A, co-expressed with EGFP (lanes 1,2,6 and 7), with P2X7A, co-expressed with 13B (lanes 3 and 8), and 13B variants expressed alone (lanes 4, 5 and 9). The numbers in brackets indicate the ratios of total protein loaded into each lane (e.g. total protein loaded in lane 1 was 50% of that loaded in lane 3). Following densitometric analysis, approximate values for expression levels are as follows: total and surface expression of P2X7A receptors were reduced to ~40% when co-expressed with the 13B variants. Similarly, total and surface expression of the 13B variant was reduced to ~50% in the presence of P2X7A receptors. Similar results were obtained in a separate experiment.

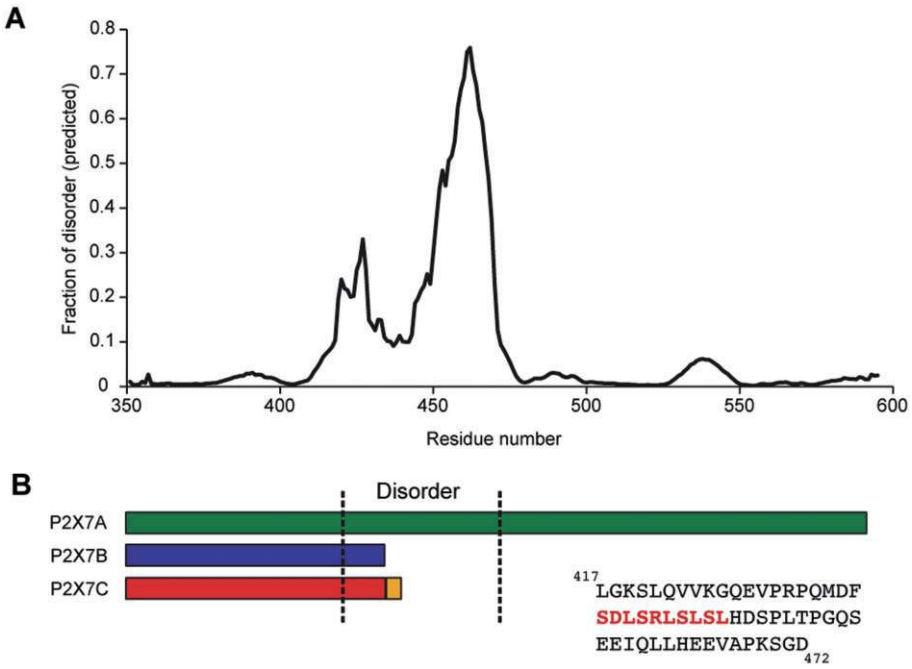

Figure 8

P2X7 ΔC variants lack disordered regions. (A) DISOPRED-2 prediction of protein disorder (lack of persistent secondary structure elements) in the C-terminal domain of P2X7 receptors. (B) Comparison of the C-terminal domains of P2X7 variants studied in this work. Note how P2X713B and P2X713C lack the most disordered region, generally associated with protein–protein interaction motifs, as identified by ANCHOR (highlighted in red).

up-regulated in pathological conditions and that they might play a role in suppressing normal P2X7 receptor function.

This study is not the first report of P2X7 receptor expression in the Pfizer KO mice. Sanchez-Nogueiro *et al*. (2005) reported the expression of P2X7 mRNA and immunoreactivity in the brain of these mice; bands running at 77 and 65 kDa were detected at similar intensity to WT brain using the anti-C term Ab, which should not recognize the 13B/C splice variants. This does not correspond in molecular mass to the P2X7 bands that we observed in spleen and SG using the extracellular Ab. By BN-PAGE analysis, we also observed a band in Pfizer brain samples using the anti-C-term Ab, but because this same band was not present when we probed with the anti-EC Ab, and did not dissociate in the presence of low concentration of SDS, we conclude that this represents non-specific binding to another protein.

Two previous studies have analysed P2X7 receptor responses in mouse SG by comparing WT and Pfizer KO glands (Nakamoto *et al*., 2009; Novak *et al*., 2010). Both report impairment in P2X7 receptor signalling in the KO glands, as we would predict based upon the low surface expression and function of the ΔC P2X7 variants. Nakamoto *et al*. (2009) showed that BzATP-stimulated salivation was reduced by ~75% in the submandibular glands of the KO mice and that the ATP-evoked rise in $[Ca^{2+}]_i$ was substantially reduced in amplitude. Novak *et al*. (2010) similarly showed a reduction in salivary secretions in the KO mice but they reported that the ATP-induced rise in $[Ca^{2+}]_i$ in SGs from WT and KO mice were similar, whereas pancreatic cells from KO animals gave a significantly reduced Ca^{2+} response compared with WT cells. Our results suggest that these residual responses to ATP and BzATP in the SG from Pfizer KO mice could be attributed to the expression of the ΔC P2X7 variants. The generation of true P2X7-null mice and further analysis of these responses would discriminate between a role for these variants versus other P2 receptors.

The C-terminal domain of P2X7 receptors has been found to confer functional specificity to the receptor via protein–protein interactions. For the 13B/C splice variants, the truncation of the C-terminal domain occurs at an interesting position with regards its structure. Within this 240 amino acid region, the stretch of amino acids immediately downstream of the deletion (431–472) is predicted to be intrinsically disordered (i.e. devoid of persistent secondary structure) (Figure 8). Intrinsic disorder has been recognized to play a key role in the specialization of protein functionality, allowing proteins to adopt multiple conformations to bind numerous partners (Meszaros *et al*., 2009). Indeed, the P2X2 receptor is functionally regulated by the protein Fe65, which binds the C-terminus of the receptor in a proline-rich region predicted to be fully disordered (Masin *et al*., 2006). A P2X2 splice variant lacking this disordered region does not interact with Fe65 and displays altered functional properties. It will be particularly interesting to find protein partners of the disordered stretch of residues identified in P2X7 receptors, which could shed more light into the different functional phenotypes observed in KO mice.

Acknowledgement

This work was supported by Biotechnology and Biological Sciences Research Council Grant BB/F001320/1 to R.M-L and by the EU Interreg IV (AdMiN) grant to DCG.

Conflicts of interest

There are no conflicts of interest.

References

Adinolfi E, Pizzirani C, Idzko M, Panther E, Norgauer J, Di Virgilio F *et al.* (2005). P2X(7) receptor: death or life? Purinergic Signal 1: 219–227.

Adinolfi E, Cirillo M, Woltersdorf R, Falzoni S, Chiozzi P, Pellegatti P *et al.* (2010). Trophic activity of a naturally occurring truncated isoform of the P2X7 receptor. FASEB J 24: 3393–3404.

Adriouch S, Dox C, Welge V, Seman M, Koch-Nolte F, Haag F (2002). Cutting edge: a natural P451L mutation in the cytoplasmic domain impairs the function of the mouse P2X7 receptor. J Immunol 169: 4108–4112.

Alexander SPH, Mathie A, Peters JA (2011). Guide to Receptors and Channels (GRAC), 5th edition. Br J Pharmacol 164 (Suppl. 1): S1–S324.

Antonio LS, Stewart AP, Xu XJ, Varanda WA, Murrell-Lagnado RD, Edwardson JM (2011). P2X4 receptors interact with both P2X2 and P2X7 receptors in the form of homotrimers. Br J Pharmacol 163: 1069–1077.

Armstrong JN, Brust TB, Lewis RG, MacVicar BA (2002). Activation of presynaptic P2X7-like receptors depresses mossy fiber-CA3 synaptic transmission through p38 mitogen-activated protein kinase. J Neurosci 22: 5938–5945.

Boumechache M, Masin M, Edwardson JM, Gorecki DC, Murrell-Lagnado R (2009). Analysis of assembly and trafficking of native p2x4 and p2x7 receptor complexes in rodent immune cells. J Biol Chem 284: 13446–13454.

Cheewatrakoolpong B, Gilchrest H, Anthes JC, Greenfeder S (2005). Identification and characterization of splice variants of the human P2X7 ATP channel. Biochem Biophys Res Commun 332: 17–27.

Chessell IP, Hatcher JP, Bountra C, Michel AD, Hughes JP, Green P *et al.* (2005). Disruption of the P2X7 purinoceptor gene abolishes chronic inflammatory and neuropathic pain. Pain 114: 386–396.

Di Virgilio F (1995). The P2Z purinoceptor: an intriguing role in immunity, inflammation and cell death. Immunol Today 16: 524–528.

Dosztanyi Z, Meszaros B, Simon I (2009). ANCHOR: web server for predicting protein binding regions in disordered proteins. Bioinformatics 25: 2745–2746.

Feng YH, Li X, Wang L, Zhou L, Gorodeski GI (2006). A truncated P2X7 receptor variant (P2X7-j) endogenously expressed in cervical cancer cells antagonizes the full-length P2X7 receptor through hetero-oligomerization. J Biol Chem 281: 17228–17237.

Ferrari D, Chiozzi P, Falzoni S, Hanau S, Di Virgilio F (1997a). Purinergic modulation of interleukin-1 beta release from microglial cells stimulated with bacterial endotoxin. J Exp Med 185: 579–582.

Ferrari D, Wesselborg S, Bauer MK, Schulze-Osthoff K (1997b). Extracellular ATP activates transcription factor NF-kappaB through the P2Z purinoreceptor by selectively targeting NF-kappaB p65. J Cell Biol 139: 1635–1643.

Gu BJ, Zhang W, Worthington RA, Sluyter R, Dao-Ung P, Petrou S *et al.* (2001). A Glu-496 to Ala polymorphism leads to loss of function of the human P2X7 receptor. J Biol Chem 276: 11135–11142.

Gu BJ, Saunders BM, Jursik C, Wiley JS (2010). The P2X7-nonmuscle myosin membrane complex regulates phagocytosis of nonopsonized particles and bacteria by a pathway attenuated by extracellular ATP. Blood 115: 1621–1631.

Guo C, Masin M, Qureshi OS, Murrell-Lagnado RD (2007). Evidence for functional P2X4/P2X7 heteromeric receptors. Mol Pharmacol 72: 1447–1456.

Hughes JP, Hatcher JP, Chessell IP (2007). The role of P2X(7) in pain and inflammation. Purinergic Signal 3: 163–169.

Humphreys BD, Dubyak GR (1996). Induction of the P2z/P2X7 nucleotide receptor and associated phospholipase D activity by lipopolysaccharide and IFN-gamma in the human THP-1 monocytic cell line. J Immunol 157: 5627–5637.

Ke HZ, Qi H, Weidema AF, Zhang Q, Panupinthu N, Crawford DT *et al.* (2003). Deletion of the P2X7 nucleotide receptor reveals its regulatory roles in bone formation and resorption. Mol Endocrinol 17: 1356–1367.

Khakh BS, North RA (2006). P2X receptors as cell-surface ATP sensors in health and disease. Nature 442: 527–532.

Labasi JM, Petrushova N, Donovan C, McCurdy S, Lira P, Payette MM *et al.* (2002). Absence of the P2X7 receptor alters leukocyte function and attenuates an inflammatory response. J Immunol 168: 6436–6445.

MacKenzie A, Wilson HL, Kiss-Toth E, Dower SK, North RA, Surprenant A (2001). Rapid secretion of interleukin-1beta by microvesicle shedding. Immunity 15: 825–835.

Masin M, Kerschensteiner D, Dumke K, Rubio ME, Soto F (2006). Fe65 interacts with P2X2 subunits at excitatory synapses and modulates receptor function. J Biol Chem 281: 4100–4108.

Meszaros B, Simon I, Dosztanyi Z (2009). Prediction of protein binding regions in disordered proteins. Plos Comput Biol 5: e1000376.

Moore SF, MacKenzie AB (2007). Murine macrophage P2X7 receptors support rapid prothrombotic responses. Cell Signal 19: 855–866.

Murrell-Lagnado RD, Qureshi OS (2008). Assembly and trafficking of P2X purinergic receptors (review). Mol Membr Biol 25: 321–331.

Nakamoto T, Brown DA, Catalan MA, Gonzalez-Begne M, Romanenko VG, Melvin JE (2009). Purinergic P2X7 receptors mediate ATP-induced saliva secretion by the mouse submandibular gland. J Biol Chem 284: 4815–4822.

Nicke A, Kuan YH, Masin M, Rettinger J, Marquez-Klaka B, Bender O *et al.* (2009). A functional P2X7 splice variant with an alternative transmembrane domain 1 escapes gene inactivation in P2X7 knock-out mice. J Biol Chem 284: 25813–25822.

North RA (2002). Molecular physiology of P2X receptors. Physiol Rev 82: 1013–1067.

Novak I, Jans IM, Wohlfahrt L (2010). Effect of P2X(7) receptor knockout on exocrine secretion of pancreas, salivary glands and lacrimal glands. J Physiol 588 (Pt 18): 3615–3627.

Pelegrin P, Surprenant A (2006). Pannexin-1 mediates large pore formation and interleukin-1beta release by the ATP-gated P2X7 receptor. Embo J 25: 5071–5082.

Roberts JA, Vial C, Digby HR, Agboh KC, Wen H, Atterbury-Thomas A *et al.* (2006). Molecular properties of P2X receptors. Pflugers Arch 452: 486–500.

Sanchez-Nogueiro J, Marin-Garcia P, Miras-Portugal MT (2005). Characterization of a functional P2X(7)-like receptor in cerebellar granule neurons from P2X(7) knockout mice. FEBS Lett 579: 3783–3788.

Sanz JM, Di Virgilio F (2000). Kinetics and mechanism of ATP-dependent IL-1 beta release from microglial cells. J Immunol 164: 4893–4898.

Sharp AJ, Polak PE, Simonini V, Lin SX, Richardson JC, Bongarzone ER *et al.* (2008). P2x7 deficiency suppresses development of experimental autoimmune encephalomyelitis. J Neuroinflammation 5: 33.

Sikora A, Liu J, Brosnan C, Buell G, Chessel I, Bloom BR (1999). Cutting edge: purinergic signaling regulates radical-mediated bacterial killing mechanisms in macrophages through a P2X7-independent mechanism. J Immunol 163: 558–561.

Sim JA, Young MT, Sung HY, North RA, Surprenant A (2004). Reanalysis of P2X7 receptor expression in rodent brain. J Neurosci 24: 6307–6314.

Smart ML, Gu B, Panchal RG, Wiley J, Cromer B, Williams DA *et al.* (2003). P2X7 receptor cell surface expression and cytolytic pore formation are regulated by a distal C-terminal region. J Biol Chem 278: 8853–8860.

Solle M, Labasi J, Perregaux DG, Stam E, Petrushova N, Koller BH *et al.* (2001). Altered cytokine production in mice lacking P2X(7) receptors. J Biol Chem 276: 125–132.

Surprenant A, North RA (2009). Signaling at purinergic P2X receptors. Annu Rev Physiol 71: 333–359.

Surprenant A, Rassendren F, Kawashima E, North RA, Buell G (1996). The cytolytic P2Z receptor for extracellular ATP identified as a P2X receptor (P2X7). Science 272: 735–738.

Taylor SR, Gonzalez-Begne M, Sojka DK, Richardson JC, Sheardown SA, Harrison SM *et al.* (2009). Lymphocytes from P2X7-deficient mice exhibit enhanced P2X7 responses. J Leukoc Biol 85: 978–986.

Ward JJ, Sodhi JS, McGuffin LJ, Buxton BF, Jones DT (2004). Prediction and functional analysis of native disorder in proteins from the three kingdoms of life. J Mol Biol 337: 635–645.

Wiley JS, Dao-Ung LP, Li C, Shemon AN, Gu BJ, Smart ML *et al.* (2003). An Ile-568 to Asn polymorphism prevents normal trafficking and function of the human P2X7 receptor. J Biol Chem 278: 17108–17113.

Supporting information

Additional Supporting Information may be found in the online version of this article:

Figure S1 RT-PCR analysis of P2X7h variant expression in WT and P2X7$^{-/-}$ mouse tissues. Primer sets specific for exon 9 and then either exon 13h (upper panel) or exon 11 (lower panel) were used to identify these transcripts in tissues from the WT and Pfizer P2X7$^{-/-}$ mice. Representative gel analysis of PCR products are shown.

Figure S2 Recognition of full-length and ΔC P2X7 variants by Abs to the EC domain and proximal C-terminus. P2X7A, the 13B variant and hybrid receptor were transiently expressed in HEK293 cells, and Western blot analysis carried out following SDS-PAGE of total cell extracts using the Abs indicated.

Figure S3 The ΔC human P2X7B receptor is inefficiently trafficked to the plasma membrane. hP2X7A and hP2X7B receptors were transiently expressed in HEK293 cells and surface biotinylation followed by Western blot analysis shows that surface expression of hP2X7B is much lower than that of the full-length P2X7A variant. The EC P2X7 Ab was used to detect both receptors.

Please note: Wiley-Blackwell are not responsible for the content or functionality of any supporting materials supplied by the authors. Any queries (other than missing material) should be directed to the corresponding author for the article.